Shock Temperature Measurement Using Neutron Resonance Spectroscopy

V. W. Yuan, J. David Bowman, D. J. Funk, G. L. Morgan, R. L. Rabie, C. E. Ragan, J. P. Quintana, and H. L. Stacy
Los Alamos National Laboratory, Los Alamos, New Mexico 87545, USA
(Received 3 September 2004; published 30 March 2005)

We report a direct measurement of temperature in a shocked metal using Doppler broadening of neutron resonances. The 21.1-eV resonance in ^{182}W was used to measure the temperature in molybdenum shocked to ~63 GPa. An explosively launched aluminum flyer produced a planar shock in a molybdenum target that contained a 1-mm thick layer doped with 1.7 at. %^{182}W. A single neutron pulse, containing resonant neutrons of less than 1 μs duration, probed the shocked material. Fits to the neutron time-of-flight data were used to determine the temperature of the shocked molybdenum.

DOI: 10.1103/PhysRevLett.94.125504 PACS numbers: 62.50.+p, 25.40.Ny, 29.30.Hs, 64.30.+t

Equation-of-state measurements are of fundamental importance in describing the behavior of materials and for applications to geophysics, astrophysics, and shock-compressed condensed-matter physics (see [1] and references therein). The equation of state (EOS) is essential in describing shock phenomena, and measurement of the shock temperature completes the EOS [2]. Previous experiments have used neutron transmission to measure temperatures under static conditions [3–5]. However, the application of this technique to shock measurements is difficult because the rarefaction-free shock state lasts only for a short time in the sample interior. To study shocked systems, neutron resonance spectroscopy (NRS) uses an intense, single pulse of neutrons to determine transient temperatures via Doppler broadening of neutron resonances in a dilute dopant. This dopant does not perturb the dynamics, and by localizing the dopant, the effects of rarefactions can be eliminated.

Successful development of the NRS technique makes possible the measurement of temperature and velocity [6] of shocked metals and detonated high explosives (HE), the temperature of shocked-induced phase transitions, and heating from friction at high-pressure, sliding interfaces. We selected molybdenum for our initial study because it is a standard in shock physics and has been extensively studied both experimentally and theoretically (e.g., see [7]). In addition, molybdenum does not have a phase change at the pressures reached in this experiment, and it forms a solid solution with a suitable dopant. In this Letter, we report the use of NRS to directly measure the internal temperature in a shocked metal.

When neutrons from a pulsed white source pass through an absorber, the time-of-flight (TOF) spectrum of the transmitted beam exhibits a series of narrow dips in the energy range below a few hundred eV. The dips, which are unique to each isotope, are caused by compound-nuclear resonances in the cross section of the absorber. For an isolated resonance, the cross section has a Breit-Wigner or Lorentzian shape and is given by

$$\sigma(E) = \frac{\sigma_0}{4} \frac{\Gamma^2}{(E - E_0)^2 + \frac{\Gamma^2}{4}}, \tag{1}$$

where E_0 is the resonance energy, E is the neutron energy relative to the target nucleus, σ_0 is the cross section at resonance, and Γ is the width. Reference [8] gives a more detailed formalism for the cross section. The thermal motion of the nuclei broadens the width of the resonance. The thermal-averaged cross section at temperature T is obtained by convolving the static cross section [Eq. (1)] with the velocity distribution $G(v, T)$ of the target nuclei:

$$\sigma(v, T) = \int_{-\infty}^{\infty} \sigma(v') G(|v - v'|, T) dv', \tag{2}$$

where $G(v, T)$ depends on the phonon distribution for a solid and transitions to a Maxwell-Boltzmann distribution at high temperatures. If target-nuclei velocities are much less than the neutron velocity, G can be well approximated by a Gaussian with a $1/e$ half-width $\Delta = 2\sqrt{(EkT/A)}$ where A is the atomic weight and k is Boltzmann's constant. Note that there is also an apparent shift in resonance energy due to bulk motion of the material.

In a dynamic temperature measurement, the thermodynamic state of the sample must remain stable during the passage of resonance-energy neutrons through the absorber. For a resonance with an energy spread ΔE, the transit time at the sample, $\Delta t_r = t\Delta E/2E_0 \sim L\Delta E/E_0^{1.5}$, is proportional to t, the time of flight to the sample, or in turn to L, the distance between the source and the sample. At Target Station 2 of the Los Alamos Neutron Science Center (LANSCE), samples can be placed less than 1 m from the neutron source, thereby shortening Δt_r to less than 200 ns FWHM.

At higher neutron energies, contributions to ΔE and Δt_r from the resonance natural width and the slowing of neutrons in the moderator (see below) are less. On the other hand, at lower energies, large cross-section resonances are more abundant, fluxes are larger, backgrounds are smaller, and our detector is more efficient. Hence the choice of

resonance is a compromise depending on the available dopants and the sample studied.

Single pulses of 800 MeV protons from the LANSCE Proton Storage Ring strike a ^{238}U target that is adjacent to a CH_2 moderator and surrounded by beryllium reflectors. Each proton pulse has a FWHM of 125 ns and produces about 5×10^{14} neutrons. The time distribution of the neutrons exiting the moderator depends on the stochastic slowing-down process in the moderator-reflector assembly. Lynn *et al.* [9] show that the time dispersion is asymmetric with a long-time tail and is representable by a weighted sum of χ^2 functions $M(t) = wf_1(t) + (1 - w)f_2(t)$, where

$$f_n(t) = \left[\frac{(t - t_n)^{(\nu_n - 2)/2}}{\Gamma(\nu_n/2)}\tau_n^{\nu_n/2}\right]e^{-(t-t_n)/t_n} \quad (t \geq t_n),$$
$$f_n(t) = 0 \quad (t < t_n), \tag{3}$$

and the τ_n and t_n scale as $1/\sqrt{E}$. By fitting well-known [10] resonances in ^{238}U, we determined (for E in eV) that $w = 0.909$, $\nu_n = 6$, $t_n = 0.11/\sqrt{E}$ μs, $\tau_1 = 0.714/\sqrt{E}$ μs, and $\tau_2 = 2.885/\sqrt{E}$ μs describe our moderator.

For the dynamic experiments, the sample and HE are contained in a steel vessel with windows 2-cm thick. The sample was positioned 0.96 m from the moderator, and neutrons transmitted through the sample are detected 23 m from the source by an array of 11 1-cm thick, 12.7-cm diam, ^{6}Li-loaded glass scintillators coupled to photomultipliers. Since the high event rate resulting from the large neutron flux precludes counting individual neutron pulses, we employed current-mode detection [11] in which we record the detector current using a transient digitizer.

In addition to prompt light emission, the ^{6}Li-glass emits a longer-lived phosphorescent component that contributes to the background signal underneath the resonances. The time dependence of the light emission was determined in measurements [12] utilizing a neutron source. We used the analytic function

$$P(t) = \sum_i \frac{\beta_i}{\tau_i} e^{-t/\tau_i}, \tag{4}$$

that spanned seven decades and 2000 μs to fit this phosphorescent data to an accuracy of about a percent.

About 400 g of PBX 9501 HE was used to launch a 6-mm thick, 63.5-mm diam cylindrical aluminum flyer [13] which traveled a free-flight distance of 15 mm and reached a velocity of $\sim$3.6 km/s before impacting the molybdenum target. This target was a 6-mm thick layered disk, 63.5 mm in diam. The 1-mm front and 4-mm rear layers were pure molybdenum. The central portion of a 1-mm thick inner layer was a 36-mm diam molybdenum disk doped with 1.7 at. %^{182}W. An outer ring of pure molybdenum surrounded the disk. A shock pressure of $\sim$63 GPa was produced in the molybdenum, and the doped disk remained at constant pressure, velocity, and temperature for about 1 μs. Figure 1(a) shows a schematic of the launcher-target assembly.

We calculate that the Hugoniot temperature for molybdenum doped with 1.7 at. % tungsten differs by only a few K from the temperature for pure molybdenum. The density of each wafer [see Fig. 1(b)], produced by arc-melting a mixture [14] of molybdenum and oxygen-free ^{182}W, was determined to an accuracy of better than 0.2%; samples used in our experiment were 10.44 and 10.43 g/cm^3, within 0.1% of full density. We estimate that this results in an increase in the Hugoniot shock temperature by at most 10 K. Metallographic analyses [15] indicate that the alloy samples were solid solutions of ^{182}W in molybdenum.

In order that the flyer not be launched toward the exit window of the containment vessel, the HE-sample assembly was tilted 55° relative to the moderator-detector axis. The detector viewed a circular region of the sample through a 30-cm long, tapered collimator with an elliptically shaped opening whose small end (2 cm $\times$ 3 cm) was located 10 cm from the sample. Rarefactions from the periphery of the sample arrived at the viewed region simultaneously.

We have analyzed data from two experiments. Figure 2(a) shows the TOF spectra for one of the experiments. The upper curve is an average of five room-temperature spectra taken prior to detonating the HE. The 21.1-eV resonance is indicated in the figure, and the dip at about 385 μs is the 18.8-eV resonance in ^{186}W, which is a small contaminant in the ^{182}W.

The lower curve shows a spectrum taken during the shock loading of the sample. The neutron flux after detonation is considerably lower than it is before the detonation because of explosive products in the neutron beam.

When the shock front passes a given position, the material behind the front is subject to a one-dimensional strain and may be briefly out of equilibrium, but within a few lattice vibrations ($< 10^{-13}$ s) any anisotropy equilibrates. The neutrons corresponding to the 21.1-eV resonance pass through the ^{182}W-doped region of the sample in the micro-

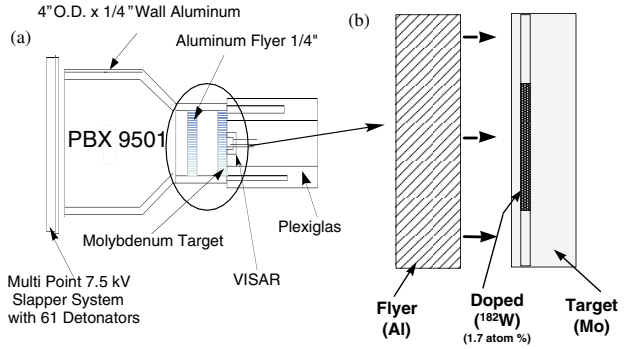

FIG. 1 (color). (a) A schematic of the launcher-target assembly. (b) A magnified view of the portion with the aluminum flyer and the target.

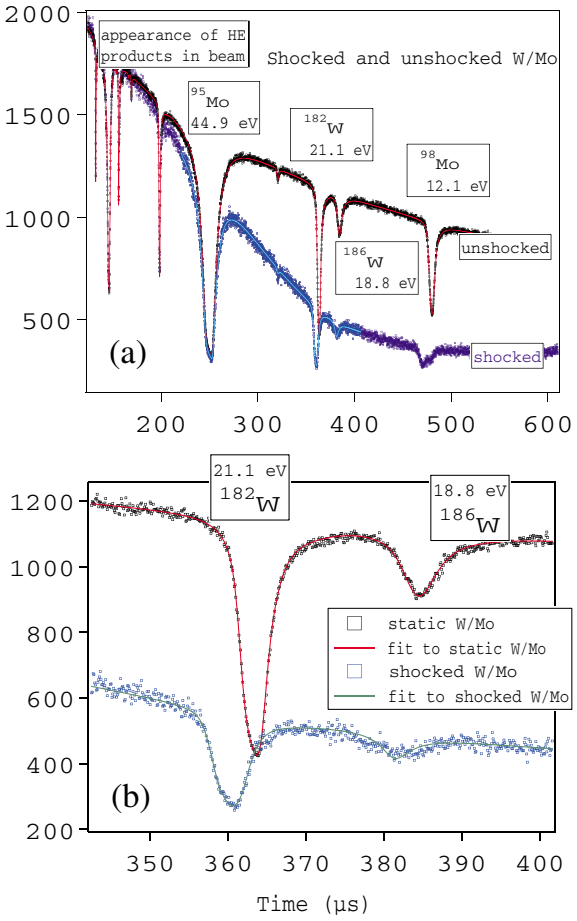

FIG. 2 (color). (a) Static (upper) and dynamic (lower) TOF spectra for shocked molybdenum. (b) Expanded view of data with fits (red and green curves) to the data. The horizontal scale for both (a) and (b) is time in microseconds.

second of stability before rarefactions perturb this region. The neutrons in the 18.8 eV resonance arrive after rarefactions, and the resonance is washed out in the lower curve.

Independent measurements using optical interferometry [16] viewing the back surface of the molybdenum determined the time of shock breakout and the time of proton beam arrival. From these results, we were able to confirm the arrival time of resonance neutrons relative to the passage of the shock in the doped region of the sample and determine the particle velocity behind the shock. Errors were assigned from variations in these signal levels.

Figure 2(b) shows the data of Fig. 2(a) on an expanded scale, along with the results of least-squares fits to the preshock and postshock data. The form of the fitting function is given by

$$Y(t) = [(\text{flux}e^{-n\sigma(v,T)}) \otimes M(t) + B] \otimes P(t), \qquad (5)$$

where $\otimes$ represents the convolution operation, $\sigma(v, T)$ is the Doppler-broadened cross section, $M(t)$ is the contribution from moderator dispersion [see Eq. (3)], B is the time-dependent background, and $P(t)$ is the contribution from phosphorescence [Eq. (4)]. The cross section was calculated using tungsten resonance parameters taken from Werner [17]. Since the moderator parameters vary with energy, a transformation in parameter space was performed in the analysis to calculate the dispersion effect as an energy-independent convolution.

Most of the neutrons in the 21.1-eV ^{182}W resonance reach the sample while it is in a shocked state. The small number of resonant neutrons that are emitted from the moderator at late times and that reach the doped region after the arrival of rarefactions can vary from one edge of the beam to the other because of the tilt of the sample relative to the beam direction. We modeled this effect by dividing the sample into different segments (each a different distance from the neutron source), and for each segment we estimated the small fraction of resonant neutrons that pass through the sample after it has been released. After studying the variation in the temperature for different assumed conditions of the released material, we found the effect on temperature to be much smaller than the statistical error.

In a set of static runs, we used NRS to measure the temperature in a natural tungsten foil that was heated in an oven, and a thermocouple read the temperature of the foil. Measurements were performed at thermocouple readings of 301, 625, and 929 K . The extracted temperatures were 310 ± 12, 612 ± 12, and 945 ± 16 K, respectively, in agreement with the thermocouple values. The good agreement places an upper limit on systematic errors and indicates that in the dynamic shots, background uncertainties are the main sources of possible systematic errors.

Temperatures derived from fits to the data of the two shots are presented in rows 1 and 2 of Table I. The combined error adds statistical errors (in parentheses) with systematic errors. We determine the latter by changing the background when fitting the dynamic data; the amount of change was determined by varying fitting regions of the static data.

Figure 3 compares the experimental result with theoretical Hugoniot temperatures derived from the Mo-2984 tables in the SESAME EOS library [18]. The displayed weighted average (see Table I) of the measured temperatures is calculated by shifting both data points to the

TABLE I. Summary of results from two shots at 63 GPa.

Data set	Particle velocity (km/s)	T(K)[a]
Shot 1	0.95 ± 0.02	786 ± 83 (66)
Shot 2	0.98 ± 0.02	926 ± 55 (24)
Wt. avg.	0.97 ± 0.02	875 ± 46
Theory	0.97	635

[a]Errors shown combine systematic and statistical (given in parentheses) contributions.

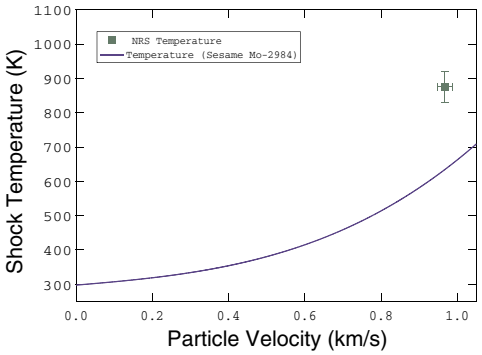

FIG. 3 (color). Comparison of NRS measured shock temperature in molybdenum with a theoretical calculation based on Mo-2984 tables in the SESAME EOS library [18].

average velocity and making the small adjustments (about 15 K) to their values based on the dependence of the theoretical curve on velocity.

The SESAME theoretical temperatures are obtained by solving the Rankine-Hugoniot jump conditions using a complete equation of state based on models for the $T = 0$ isotherm, lattice vibrations, and electronic excitations [19]. In the models [20] used, the specific heat is dominated by the contribution of lattice vibrations $3R$, where R is the ideal gas constant. Within experimental constraints, Greeff [21] has investigated the effect of uncertainties in model parameters, such as the vibrational Gruneisen parameter and electronic density of states under compression. The calculated temperature varies by roughly 30 K at 63 GPa based on these uncertainties. The measured temperature is significantly higher than the theoretical prediction. Similar discrepancies have been observed [22,23] at lower pressures and were attributed by one set of authors [23] to elastoplastic work, but these effects should be small at the pressures of our measurement. The disagreement between our measurements and theoretical calculations is presently not understood, but the discrepancy can be investigated by shock temperature measurements in other metals.

In summary, neutron resonance spectroscopy has been used to make a direct measurement of the temperature behind a shock. Through selective dopant placement, the interior temperature during dynamic loading has been determined essentially free of rarefactions and release waves. The measured temperature deviates significantly from theoretical predictions, and this disagreement needs further investigation. We have demonstrated that NRS can be used for shock physics studies and in a wide variety of other applications.

The authors wish to thank Carl Greeff of the Theoretical Division at Los Alamos National Laboratory, Gregg Chaparro and Lloyd Hunt of the LANSCE Division, and Adam Whiteson of Bechtel Los Alamos. This work was performed under the auspices of the U.S. Department of Energy under Contract No. W-7405-ENG-36. Funding for this work was provided by DOE/DP.

[1] R. Cauble *et al.*, Phys. Rev. Lett. **80**, 1248 (1998).
[2] Y. Zhao *et al.*, Phys. Rev. B **62**, 8766 (2000).
[3] P. H. Fowler and A. D. Taylor, Los Alamos National Laboratory Conference Report No. LA-11393-C, 1987.
[4] J. Mayers, G. Baciocco, and A. C. Hannon, Nucl. Instrum. Methods Phys. Res., Sect. A, **275**, 453 (1989).
[5] Y. Le Godec *et al.*, Mineral. Mag. **65**, 737 (2001).
[6] C. E. Ragan III, M. G. Silbert, and B. C. Diven, J. Appl. Phys. **48**, 2860 (1977).
[7] R. S. Hixson and J. N. Fritz, J. Appl. Phys. **71**, 1721 (1992).
[8] C. W. Reich and M. S. Moore, Phys. Rev. **111**, 929 (1958).
[9] J. E. Lynn *et al.*, Phys. Rev. B **58**, 11 408 (1998).
[10] S. F. Mughabghab, M. Divadeenam, and N. E. Holden, *Neutron Cross Sections*, (Academic, New York, 1981), Vol. 1, Part B.
[11] J. D. Bowman *et al.*, Nucl. Instrum. Methods Phys. Res., Sect. A **297**, 183 (1990).
[12] V. Yuan, J. D. Bowman, G. L. Morgan, and S. Penttila, Los Alamos National Laboratory Report No. LA-UR-00-145, 2000.
[13] C. A. Forest, R. L. Rabie, L. Bennett, and J. Vorthman, in *Proceedings of the 11th International Symposium on Detonation, Snowmass, CO, 1988* (Office of Naval Research Report No. ONR 3300-5, 1998).
[14] S. R. Bingert, P. B. Desch, and E. Trujillo, *Proceedings of the 1989 International Conference on Powder Metallurgy and Particulate Materials*, (MPI Federation, Princeton, 1999).
[15] S. R. Bingert (private communication).
[16] L. M. Barker and R. E. Hollenbach, J. Appl. Phys. **43**, 4669 (1972).
[17] C. J. Werner, Ph.D. thesis, Rensselaer Polytechnic Institute, 1998.
[18] S. P. Lyon and J. D. Johnson, Los Alamos National Laboratory Report No. LA-UR-92-3407, 1992.
[19] E. D. Chisolm, S. D. Crockett, and D. C. Wallace, Los Alamos National Laboratory Report No. LA-UR-03-4928 (submitted to APS SCCM Conference Proceedings), 2003.
[20] D. C. Wallace, *Statistical Physics of Crystals and Liquids*, (World Scientific, River Edge, NJ, 2002).
[21] C. Greeff (private communication).
[22] W. G. Von Holle and J. J. Trimble, J. Appl. Phys. **47**, 2391 (1976).
[23] S. A. Raikes and T. J. Ahrens, Geophys. J. R. Astron. Soc. **58**, 717 (1979).